



A measurement of the photonuclear interactions of 180 GeV muons with the TILECAL Module 0 and prototypes

TILECAL Collaboration

R. Leitner

Charles University, Prague, Czech Republic

Abstract

The energy spectrum and the cross section of photonuclear interactions of 180 GeV muons in iron has been measured with the setup of the Module 0 and prototypes of the ATLAS hadron calorimeter in the H8 beam of the CERN SPS.

The differential cross section $(N_A/A)v d\sigma/dv$ of a fractional energy loss $v = \Delta E_\mu/E_\mu$ has been measured in the range $v = 0.1 \div 1$; it is compared with the theoretical predictions.

Measured value of $(0.25 \pm 0.03_{stat} \pm 0.03_{syst}) \cdot 10^{-6} cm^2 g^{-1}$ of the integrated cross section $(N_A/A) \int_{0.1}^1 v d\sigma/dv$ for was found in good agreement with the theoretical prediction of $0.267 \cdot 10^{-6} cm^2 g^{-1}$.

1 Introduction

In this paper, a measurement performed in 1998 with 180 GeV muons incident on a Module 0 of the ATLAS[1] Tile Calorimeter[2] is described and the results are compared with theoretical predictions.

The photonuclear interactions of muons have been discovered[3] in 1995. However there are only very few measurements of the photonuclear reaction with low momentum transfer [4]. As noted in [4], the photonuclear interactions of muons might produce a background in many underground experiments and it is therefore important to measure their cross section. In the paper[5] it was pointed out, that there are two different theoretical predictions which are implemented in different Monte Carlo programs. The predictions differs each from other by an order of magnitude.

2 Experiment and Data Analysis

The ATLAS Tile Calorimeter is an iron-scintillator sampling calorimeter equipped with wavelength-shifting fibre readout. An important feature of this calorimeter is that the scintillator tiles are placed perpendicular to the colliding beams; a detailed description of the calorimeter concept and of the Module0 and prototypes is given elsewhere [2]. For the purpose of this measurement, the Module 0 and prototypes of the calorimeter was placed in the H8 beam of the CERN SPS, and oriented so that particles cross the tiles at perpendicular incidence (Fig. 1). In this configuration the muon beam traverses periods of an alternating towers of iron (14 mm), scintillator (3 mm) and about 0.4 mm of other light elements (scintillator wrappings, the glue). The fibres collecting light from the scintillator are read out by photomultipliers and are grouped in such a way that sixteen calorimeter towers are defined. Each tower contains 17 to 21 periods. In the experimental set-up, 5.6 m long Module 0 was placed on three prototypes and covered by other two prototypes from the top The beam entered in the centre of the Module 0.

Particles of the momentum-analysed muon beam, with an energy $E_\mu = 180$ GeV, were triggered by three scintillator hodoscopes; the direction of incidence was measured by a pair of two-coordinate wire chambers. Approximately 400 000 muon triggers were used in this analysis.

A minimum-ionizing particle signal was required in scintillator hodoscopes in order to suppress trigger more than one entering particle.

Only events with the signal compatible with the beam spot of 1.5x1.5 cm in the beam chambers have been selected.

About 190 thousands of events have been selected for further analysis.

2.1 Selection of photonuclear events

The photonuclear events are characterized by the production of hadrons and therefore by hadronic showers. The candidates of photonuclear events have been selected by the requirement of quite large signal in the prototypes. At least one cell with the signal exceeding 0.75 GeV have been required in one of the five prototypes.

In order to ensure optimal containment of showers produced by muon photonuclear interactions, only events with maximum response between the 7-th to the 13-th tower (seen by the beam) of the calorimeter were selected. In such a way all muons which started their interaction within the region of 124 calorimeter periods are accepted.

In order to eliminate very low hadron and electron contamination of the beam, the signal in calorimeter towers preceding the interaction was required to be compatible with minimum ionizing particle, i.e. only particles which have passed 7.5 nuclear interaction lengths and 80 radiation lengths without the interaction are selected. Expected number of hadron induced interaction in analysed data sample is less than 0.5 events. The number of muon decays in flight within the acceptance region inside the calorimeter was estimated to be 1.5 event in the accepted data sample. We have find two events without muon escaping the shower and these events have been excluded from the analysis.

The energy ΔE_μ lost by muons in the calorimeter is defined in this analysis by excluding the minimum-ionization signal. It was calculated by summing the signals in five consecutive towers of the Module 0 and signal in the prototypes and subtracting the experimental value of the truncated mean of muon signal $1.7 \cdot E_{mp}$ in those towers. The hadronic energy of the shower have been expressed in the electromagnetic scale using the value of $e/h = 1.35$. The muon fractional energy loss was defined to be:

$$v = \Delta E_\mu / (E_\mu - \epsilon)$$

where the muon energy losses ϵ measured in towers preceding the interaction have been subtracted from the nominal beam energy.

The positions of maximal signals in the Module0 and prototypes was required to coincide within $\pm 700mm$.

In total 79 candidates of photonuclear interactions with $v \geq 0.1$ have been found. Typical example of the selected events is shown on Fig. 2.

2.1.1 The background

The most important sources of the background events are knock-on electron or radiative losses of muons accompanied by the signal in the prototypes. The knock-on and radiative losses of muons in the TileCal Module 0 and prototypes have been investigated in Ref.[6, 7].

There are three possible sources of signals in prototypes:

- **The Noise.** The typical value of the r.m.s. of the noise signal in prototype cells is 20 MeV. Therefore the probability it will fluctuate above 0.75 GeV is very low.
- **Cosmics rays and the beam halo.** Due to quite large integration time of the signal processing in the prototypes, the random coincidence of the cosmic rays or the beam halo particles signal in the prototypes had to be investigated. The events with the m.i.p. signal in the Module 0 have been used for this purpose. The value of the suppression of the cosmic rays signals by a factor of 10^{-3} have been found for the cutoff of 0.75 GeV for the maximal cell response in the prototypes.
- **Lateral leakage of elektromagnetic showers.**

Although the lateral dimension of calorimeter towers is about 6 Moller radii, the lateral leakage of electromagnetic showers produced in knock-on electron production and radiative muon losses appeared to be the most important source of the background.

All the types of the background have been studied using electron beams of 10 and 100 GeV. The suppression factors of $1.5 \cdot 10^{-3}$ and $4 \cdot 10^{-3}$ have been found for 10 and 100 GeV electron data respectively.

2.1.2 The Acceptance

The acceptance have been estimated using pion beams with different energies. Its values defined as the fraction of events with the maximal signal in one prototype cell being greater than 0.75 GeV are plotted on Fig. 3 together with the approximation:

$$acc(v) = 1.2254 \cdot v - 0.40246 \cdot v^2 \quad (1)$$

which have been used in further analysis.

2.2 The cross section evaluation

Two different methods have been used to evaluate the cross section.

2.2.1 Method I

At a given value of the muon fractional loss v , the observed number of events $N_{obs}(v)$ is a composition:

$$N_{obs}(v) = N_{ph}(v) \cdot acc(v) + N_{rad}(v) \cdot sup(v) \quad (2)$$

of the number $N_{ph}(v)$ of the photonuclear events measured with the acceptance $acc(v)$ and the number $N_{rad}(v)$ of knock-on electrons or radiative muon losses suppressed by a factor of $sup(v)$. A solution of the equation for the number of photonuclear events is:

$$N_{ph}(v) = \frac{N_{obs}(v)}{acc(v)} \cdot \frac{1}{1 + cont(v)} \quad (3)$$

The term $cont(v)$ is the contamination of the data:

$$cont(v) = \frac{N_{rad}(v) sup(v)}{N_{ph}(v) acc(v)} \quad (4)$$

and it is plot on Fig. 4. It has been calculated using measured values of the acceptance and suppression factors and the theoretical predictions for the different mechanisms of the muon energy losses. The lower limit of the analyzed energy loss spectrum was set to $v = 0.1$ in order the contamination would not excess 20%.

Finally the differential mean energy loss in the i -th interval was calculated as

$$\frac{N_A}{A_{Fe}} v \frac{d\sigma}{dv} = \frac{\sum_1^{N_i} v_i \cdot w(v_i)}{\Delta v_i} \frac{1}{L_{Fe} \cdot \rho_{Fe}} \frac{1}{1 + L_{sci} \rho_{sci} / L_{Fe} \rho_{Fe}} \quad (5)$$

where each event has its own weight:

$$w(v_i) = \frac{1}{acc(v_i) (1 + cont(v_i))}. \quad (6)$$

Here v_i is the measured value of v , N_i is the number of events in the i -th interval, Δv_i is the width of the i -th interval, N_A is the Avogadro number in units of mol^{-1} . The variables L_{Fe} , ρ_{Fe} and A_{Fe} are the length of the accepted region of the iron in cm, its density in $g \cdot cm^{-3}$ and atomic weight of the iron in $g \cdot mol^{-1}$ respectively. The length and the density of light materials (mainly the scintillator) are denoted by L_{sci} , ρ_{sci} .

2.2.2 Method II

An alternative method was used to analyse the data. This method used the difference of longitudinal shapes of electromagnetic and hadronic showers. The number N_{90} of consecutive layers which contains 90 % of the total shower energy deposited in the Module 0 has been calculated.

This variable is equal to $\langle N_{90} \rangle = 2$. for the electromagnetic showers. In selected data sample the same variable was equal to $\langle N_{90} \rangle = 3.5$. The difference

of the two values is a clear indication that the selected data sample contained mainly muon interactions which produced hadronic showers.

Therefore in the Method II only events with $N_{90} \geq 3$ have been selected and processed with the assumption of zero contamination coefficient $coef(v) = 0$. The difference of results obtained by Methods I and II have been added to systematic errors evaluation.

2.2.3 Systematic errors

The systematic errors of the energy loss spectrum are dominated by the uncertainty on the acceptance and suppression factors evaluation and the uncertainty in the e/h ratio. The result is an overall systematic error of $\pm 12\%$. The contributions to this value are listed in the Table 1.

3 Comparison of Experiment and Theory

The measured values of differential cross section of muon photonuclear interactions with iron are given in Table 2 and are plotted in Fig. 5. The results have been compared (see the curve on Fig. 5) to theoretical prediction calculated by [8] and given in [9]. The measured data agrees with the theoretical prediction.

Measured value $(0.25 \pm 0.03_{stat} \pm 0.03_{syst}) \cdot 10^{-6} cm^2 g^{-1}$ of the integrated cross section defined as: $(N_A/A) \int_{0.1}^1 v d\sigma/dv$ is also in very good agreement with theoretical prediction[8] of $0.267 \cdot 10^{-6} cm^2 g^{-1}$.

Acknowledgements

The construction of calorimeter Module 0 was only possible with substantial contributions by the technical staff of the collaborating institutions. We deeply thank them for their support.

Financial support is acknowledged from the funding agencies to the collaborating institutions.

Finally we are grateful to the staff of the SPS, and in particular to K. Elsener, for the excellent beam conditions and assistance provided during our tests.

References

- [1] ATLAS Collaboration, ATLAS Technical Proposal, report CERN/LHCC/94-43.
- [2] F. Ariztizabal et al., Nucl. Instrum. Methods A349 (1994) 384.
E. Berger et al., report CERN/LHCC 95-44.
Atlas Collaboration, Tile Calorimeter TDR, CERN/LHCC 96-42.

- [3] E.P. George nad J. Evans, Proc. Phys. Soc. 68 (1955) 829.
- [4] G. Battistoni et al., hep-ex/9809006, 9 Sep 1998.
- [5] G. Battistoni et al., Nucl. Instrum. Methods A394 (1997) 136.
- [6] E. Berger et al., Z. Phys. C73 (1997)455-463; CERN-PPE/96-115, CERN 1996.
- [7] R. Leitner, ATLAS Internal Note ATL-TILECAL-99-009, CERN 1999.
- [8] L.B. Bezrukov and E.V. Bugaev, Sov. J. Nucl. Phys. 33 (1981) 635.
- [9] W. Lohmann et al., CERN report 85-03 (1985).

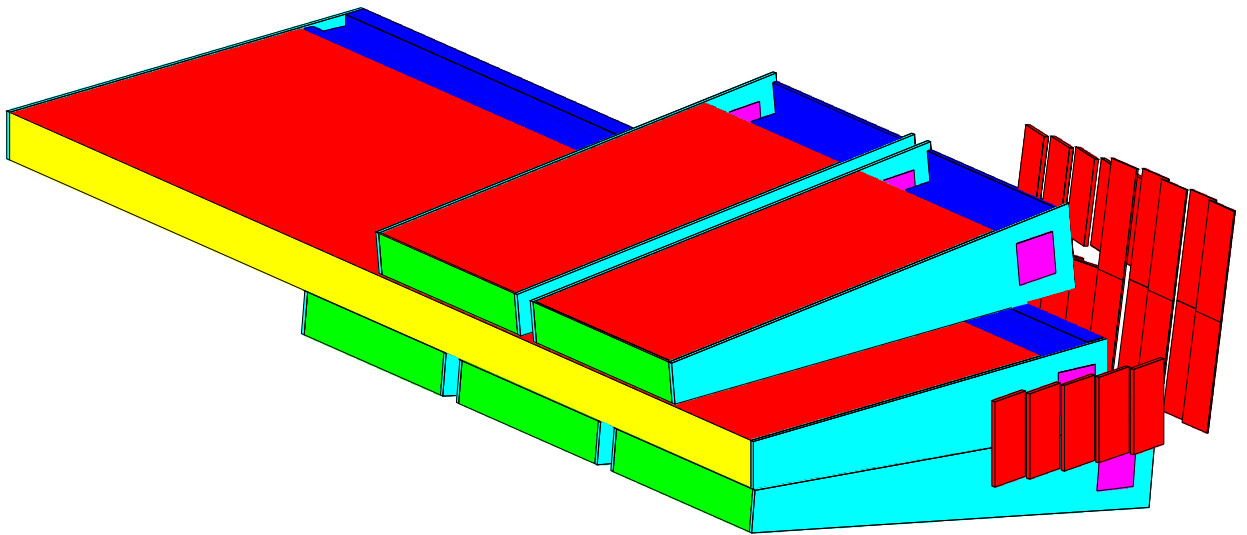


Fig. 1 The experimental setup. The beam enters the center of 5.6 m long Module 0 from the left side.

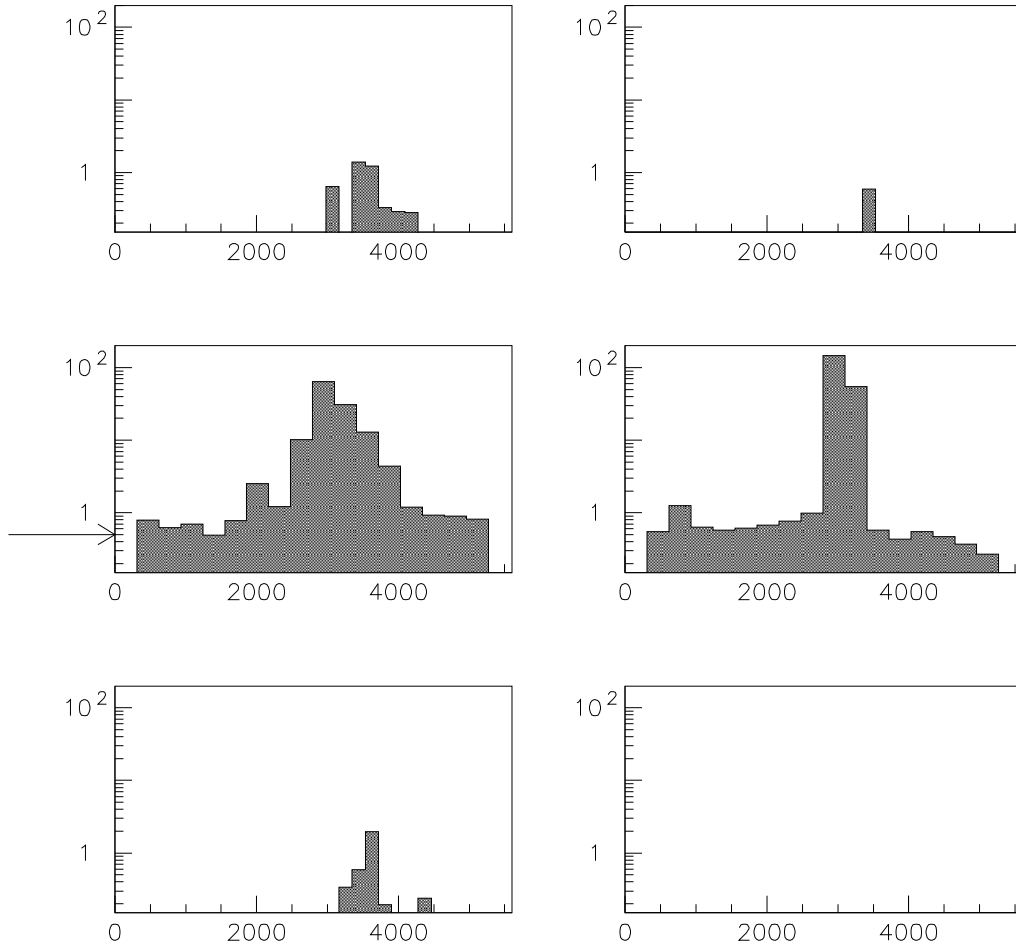


Fig. 2 The example of photonuclear interaction of muon (left plots) and the background event (right plots). The signals (in GeV) in towers (coordinates in mm) in the prototypes (upper and bottom plots) and in the Module 0 (plots in the middle) are shown. The photonuclear interactions are characterized by longer and wider showers compare to showers of the background events. The primary muon direction is indicated by the arrow.

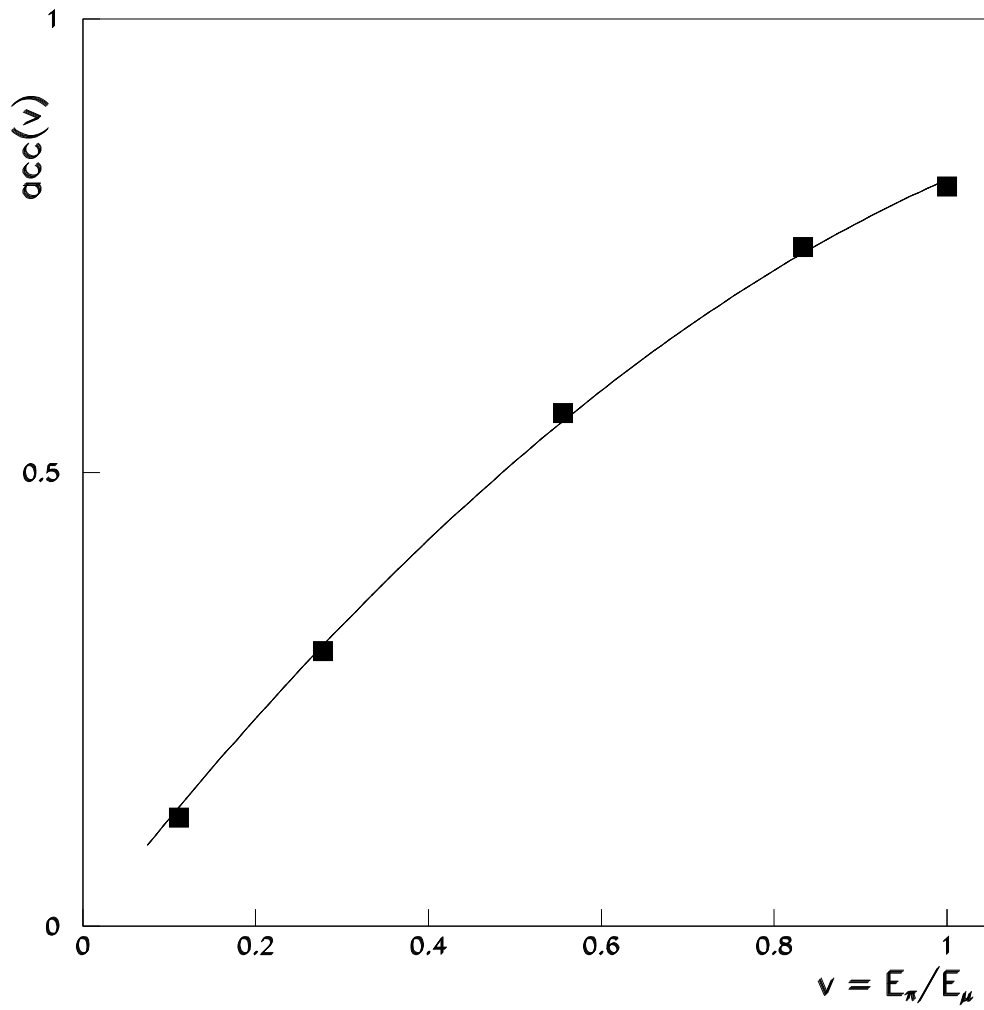


Fig. 3 The values of the acceptance of photonuclear events measured with hadron beams. The curve is the parametrization described in the text.

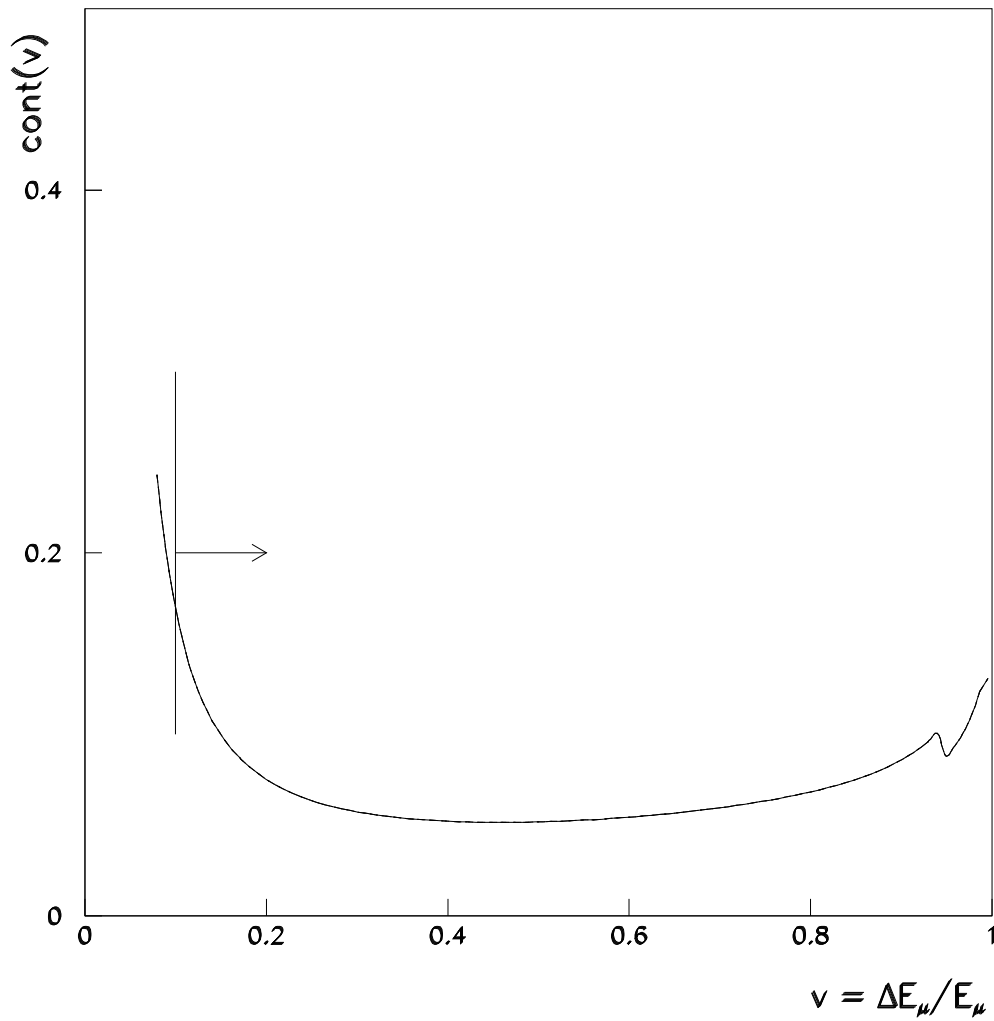


Fig. 4 The dependence of the contamination factor on muon fractional energy loss. Vertical line and the arrow indicate the region of analyzed data ($v \geq 0.1$) with the contamination lower than 20%.

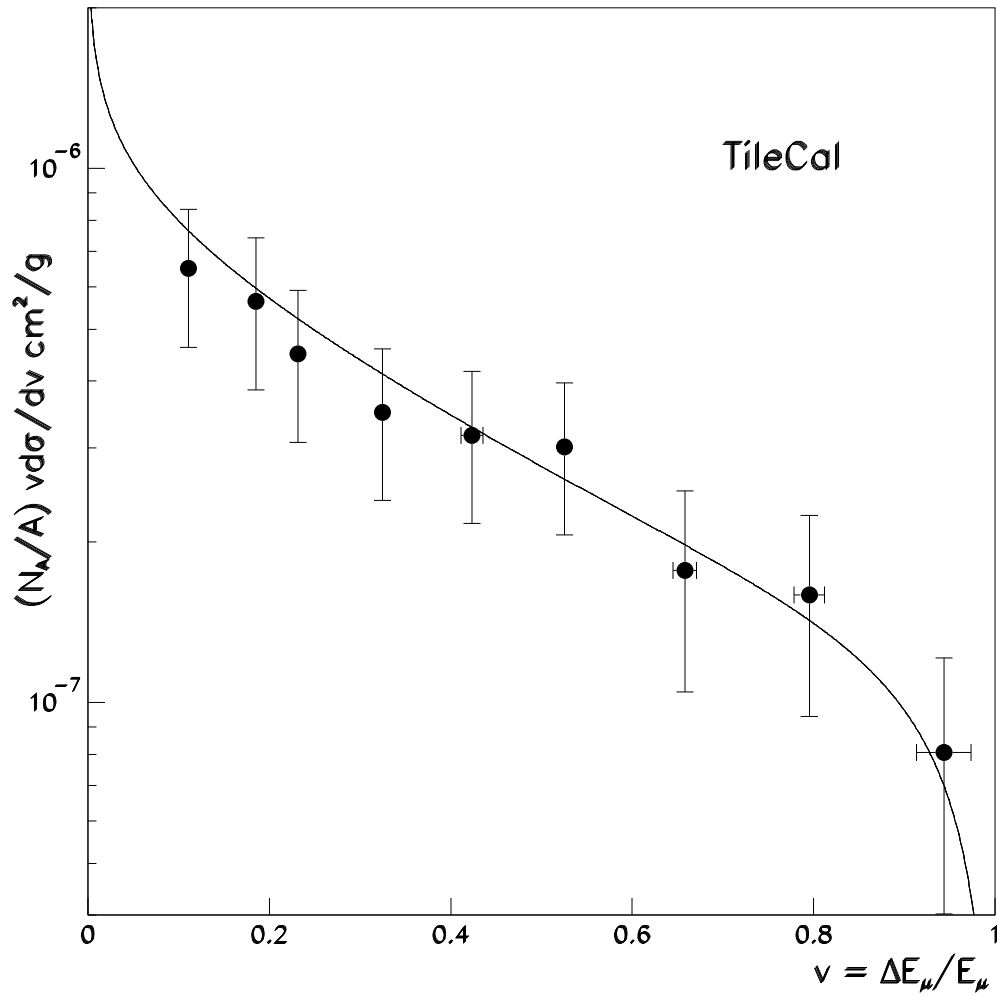


Fig. 5 Measured differential cross section of 180 GeV muon photonuclear interactions with the iron are shown by full circles. The curve is the theoretical prediction of the Ref.[8].

Table 1

The contributions to systematic errors.

| Source | Syst. error in % |
|--------------|------------------|
| e/h | 5 |
| Meth I/II | 3 |
| Acceptance | 10 |
| Energy scale | 3 |
| Total | 12 |

Table 2The measured differential cross section values $v\Delta\sigma/\Delta v$ for fractional photonuclear muon energy losses v and theoretical predictions[8].

| $\langle v \rangle$ | $(A/N_A)v d\sigma/dv (meas.)$ $cm^2 \cdot g^{-1}$ | $(A/N_A)v d\sigma/dv (th.)$ $cm^2 \cdot g^{-1}$ |
|---------------------|--|--|
| (0.110 ± 0.005) | $(0.65 \pm 0.19) \times 10^{-6}$ | 0.77×10^{-6} |
| (0.185 ± 0.005) | $(0.56 \pm 0.18) \times 10^{-6}$ | 0.60×10^{-6} |
| (0.23 ± 0.01) | $(0.45 \pm 0.14) \times 10^{-6}$ | 0.52×10^{-6} |
| (0.33 ± 0.01) | $(0.35 \pm 0.11) \times 10^{-6}$ | 0.41×10^{-6} |
| (0.42 ± 0.01) | $(0.32 \pm 0.11) \times 10^{-6}$ | 0.33×10^{-6} |
| (0.53 ± 0.01) | $(0.30 \pm 0.10) \times 10^{-6}$ | 0.26×10^{-6} |
| (0.66 ± 0.01) | $(0.18 \pm 0.07) \times 10^{-6}$ | 0.20×10^{-6} |
| (0.80 ± 0.02) | $(0.16 \pm 0.07) \times 10^{-6}$ | 0.14×10^{-6} |
| (0.94 ± 0.03) | $(0.08 \pm 0.04) \times 10^{-6}$ | 0.07×10^{-6} |